Nano-ice models for the water aggregates observed on the h-BN/Rh(111) nanomesh

Ding, Y ; Iannuzzi, M ; Hutter, J

Abstract: When a large amount of water is deposited onto a bare h-BN/Rh(111) nanomesh, the formation of ordered and stable nano-ice crystals in the pores has been experimentally observed. The present work proposes different possible models for the structure of the observed clusters, based on density functional theory calculations of two-dimensional water lattices adsorbed on free-standing hexagonal BN. Through the investigation of the electronic properties, the interaction with BN, and the distribution of the molecular dipoles, the most probable two-dimensional arrangement has been identified. Finally, a model is proposed for the nano-ice cluster trapped in the pore of the nanomesh, which constitutes 38 molecules distributed according to the most probable two-dimensional arrangement on free-standing BN. Structural and electronic properties of the optimized nano-ice cluster are also reported, and it is shown that the model is consistent with the experimental observation.

DOI: https://doi.org/10.1088/0953-8984/24/44/445002

Nano-ice Models for the Water Aggregates Observed on the *h*-BN/Rh(111) Nanomesh

Yun Ding, Marcella Iannuzzi,* and Jürg Hutter

Institute of Physical Chemistry, University of Zurich

Winterthurerstrasse 190 CH-8057 Zurich, Switzerland

Abstract

When a large amount of water is deposited onto the bare *h*-BN/Rh(111) nanomesh, the formation of ordered and stable nano-ice crystals in the pores has been experimentally observed. The present work proposes different possible models for the structure of the observed clusters, based on density functional theory calculations of two dimensional water lattices adsorbed on free-standing hexagonal BN. Through the investigation of the electronic properties, the interaction with BN, and the distribution of the molecular dipoles, the most probable two-dimensional arrangement has been identified. Finally, a model is proposed for the nano-ice cluster trapped in the pore of the nanomesh, which is constituted of 38 molecules distributed according to the most probable two-dimensional arrangement on free-standing BN. Structural and electronic properties of the optimized nano-ice cluster are also reported, and it is shown that the model is consistent with the experimental observation.

*Electronic address: marcella@pci.uzh.ch

I. INTRODUCTION

The boron nitride nanomesh is the superstructure formed by epitaxially growing hexagonal BN on Rh(111) surface[1, 2]. The lattice mismatch between the two materials induces the modulation of the interaction between BN and the metal. Where N atoms are located on top of Rh atoms, stronger electronic interaction is possible and the BN overlayer tends to stay close to the metal, at about 2.2 Å[3]. Elsewhere, the interaction is weak and the overlayer remain farther, at about 3.1 Å from the substrate[3]. The BN height variation creates depressions of 2 nm of diameter[1, 2], which are called pores, while the weakly bound regions form a connected network, called wire. The resulting superstructure has a periodicity of 3.2 nm and is called nanomesh. The nanomesh is quite stable in gas phase[4], liquid water[2], and other organic solvents[5]. It has been experimentally observed that adsorbed molecules can be trapped in the pores[1, 2, 6], thus making it an interesting template for self-assembly of distant and ordered molecular arrays, or even as base-structure for fundamental studies of two-dimensional confined structures.

In our previous works[3, 7, 8], we have described small aggregates of water molecules adsorbed on the nanomesh when little amount of water is deposited. We have optimized and characterized the structure and the electronic properties of several water clusters (up to 6 molecules) located in the pore and on the wire of the nanomesh. We could also determine that the triple protrusions appearing in the experimental scanning tunneling microscopy (STM) images are, most probably, water hexamers.

Experiments also show that by increasing the amount of water deposited to the nanomesh at low temperature (52 K), larger aggregates are formed and fill the entire pore[6]. From the detailed inspection of the STM images and the corrugation profile, it has been determined that the aggregates contain about 40 molecules which form honey-comb like lattices. The molecules are distributed over two sub-lattices (A and B), which give rise to different contrast in the STM image. The modulation of the brightness has been interpreted as different height of the A and B molecules over the substrate. This interpretation is in agreement with the results obtained for the small water clusters adsorbed in the nanomesh pore, where the STM image of the hexamer shows brighter contrast for the molecules forming a hydrogen bond with the substrate and exposing the O lone pair outwards[3, 7]. On the other hand, the fact that STM cannot resolve well-defined structures on the wire has been interpreted with high mobility of the extremely weakly adsorbed molecules.

The formation of bilayer aggregates of water molecules on solid surfaces, with structure size

ranging from small clusters to full monolayers, has been already reported in numerous previous works[9–18]. Understanding the role of the substrate on the water clustering and on possible ice nucleation processes is considered a challenging and fundamental question, which has been addressed many times using both experimental and theoretical investigation tools[9–18]. In particular, the cooperativity between surface bonding and hydrogen bonding has been identified as a crucial factor that underlies the stability of the formed structures at metal surface. Moreover, buckled layers of water molecules have been associated to different interaction types thus distinguishing in between low lying and high lying molecules as two different molecule types.

In this work, we discuss the properties of water arrays on *h*-BN, which is a hydrophobic substrate offering different adsorption sites. Although hydrogen bond could be formed between water and N atoms in the *h*-BN layer, the binding energies among water molecule themselves are much stronger compared to the adsorption energy between water and the substrate according to our previous work[3] as well as the results of nanoice clusters reported here. Thus, water molecules would always tend to form aggregates instead of being separated on a *h*-BN layer, which is the reason why we consider the *h*-BN layer as hydrophobic. The structures considered here are also obtained by the characteristic water hexamer as building block, and focus is set on how the adsorption site and the distribution of molecular orientation can affect the stability. These features are closely related to the properties of the hydrogen bond network, including also hydrogen bond to the substrate. As a first step, we consider simple systems constituted of a flat and free-standing *h*-BN layer fully covered by the water array. According to the experimental observation[6], the water lattice has to be honeycomb-like with two sublattices, the O-O second neighbor distance has to be close to the one characteristic of hexagonal ice, i.e. 4.6 Å. The structural optimizations starting from different initial configurations have revealed quite a number of possible stable arrays, which differ in the location of the molecules over the substrate, the height of the overlayer, the corrugation defined as the height difference between the two sublattices, the relative orientation of the water molecules, and the distribution of the hydrogen bonds. Finally, from the analysis of the optimized models, we could identify the best candidate to reproduce the nano-ice cluster observed by the STM experiments. We report results of the optimization of the selected water cluster constituted of 38 water molecules when it is located within the pore of the full nanomesh substrate. It is shown that the optimized structure agrees with the experimental findings.

II. METHOD

All the calculations are carried out with the CP2K program package[19] applying the hybrid Gaussian and plane waves (GPW) method[20]. We used revised PBE[21, 22] for the exchange and correlation functional in all the DFT calculations, and an additional Grimme potential[23] is added in order to include van der Waals dispersion corrections. Goedecker-Teter-Hutter (GTH) pseudopotentials[24–26] are used to approximate the interaction of the valence electrons with atomic cores. A large core pseudopotential and nine valence electrons with a single zeta basis set have been used for Rh. Double zeta short range molopt basis sets[27] are employed for B and N, while triple zeta basis sets are used for O and H. For the calculation with the nanomesh, we used a 13 $\times$ 13 BN layer with a four-layer 12 $\times$ 12 Rh slab, which represents the full unit cell of the nanomesh. Periodic boundary conditions are always applied in the calculations, and all the reported energy differences are corrected for the basis set superposition error (BSSE) using Boys and Bernardi counterpoise method[28]. STM simulations have been carried out within the Tersoff-Hamann approximation[29, 30], following the same procedure described in Ref.[3]. The molecular dipole moments are computed as

$$p = \sum_i q_i^n \vec{r}_i^n + \sum_k q_k^w \vec{r}_k^w, \tag{1}$$

where q^n and $\vec{r}^n$ are charge and position of the nuclei, whereas q^w and $\vec{r}^w$ are charge (-2e) and position of the center of the maximally localized Wannier functions (MLWF) representing the electronic structure of the adsorbed molecules. The MLWF are obtained for each optimized geometry minimizing the total spread of the molecular orbitals[31]. For each water molecule, one MLWF center is located along every OH bond and represents the electron pair, while two more MLWF centers represent the position of the O lone pairs.

The energetics of the optimized structures are compared in terms of the adsorption energy per water molecule E_{ads}, the interaction energy per water molecule E_{int}, and the hydrogen bonding contribution $E_{\text{H-bond}}$. E_{ads} is defined as the total energy of the optimized structure E_{M} minus the energy of the optimized free-standing BN layer and N-times the energy of one water molecule in gas phase, where N is the number of water molecules in the simulation box, and then divided by N, $E_{\text{ads}} = (E_{\text{M}} - (E_{\text{BN}} + N \times E_{\text{H}_2\text{O}}))/N$. E_{int} is defined as the total energy of the optimized structure minus the energy of the optimized free-standing BN layer and the energy of the optimized free-standing monolayer of water molecules, then divided by N, $E_{\text{int}} = (E_{\text{M}} - (E_{\text{BN}} + E_{\text{iceML}}))/N$.

$E_{\text{H-bond}}$ is the difference between E_{ads} and E_{int} divided by $\frac{3}{2}$, since each molecule in the water monolayer forms three hydrogen bonds with neighboring molecules and we need to cancel the double counting by times the factor $\frac{1}{2}$.

III. STRUCTURAL MODELS ON FLAT BN

By considering the structural requirements suggested by the experimental analysis, three possible two dimensional arrangements of the water O atoms over the BN layer are proposed. The three resulting oxygen lattices are depicted in FIG. 1, as model M1, model M2, and model M3. In the figure the red circles and the green diamonds indicate the sublattices A and B, respectively, while the black lines represent the vectors of the hexagonal unit cell.

Model M1 is a $\sqrt{13} \times \sqrt{13}$ structure with 8 atoms per unit cell. One every four O belonging to the sublattice A is located on top of the BN ring-center, whereas in the sublattice B, one every four O occupies a N-top site. The lattice constant is $a_0 = 9.2$ Å, which corresponds to a second neighbor O–O distance of 4.6 Å, while the closest distance is 2.66 Å. The O lattice is rotated with respect to the BN lattice by an angle of 13.9°.

Model M2 is a 2×2 structure, with lattice constant of 5.1 Å and two O per unit cell. It can also be represented by an orthogonal cell, indicated by the dashed magenta lines in FIG. 1, and containing 4 O atoms. In this configuration, the O–O distances are a bit larger, being 2.95 Å for the first neighbors and 5.1 Å for the second neighbors. The M2 lattice has the same orientation as the BN lattice.

Model M3 is a $\sqrt{3} \times \sqrt{3}$ structure where all the O atoms occupy N-top sites. The unit cell contains two molecules and $a_0 = 4.42$ Å. The smallest orthogonal cell, instead, contains four molecules and is shown in the figure by the magenta lines. The O–O nearest neighbor distance is 2.55 Å and the rotation angle with respect to the BN lattice is of 30°.

The calculations starting from the M1 configuration have been carried out using a 3×3 hexagonal supercell containing 72 water molecules. For the other two models, orthorhombic cells have been used. A 4×2 supercell for M2, containing 32 water molecules, and a 3×4 supercell for M3, containing 48 molecules.

The stability and the electronic properties of the water array are expected to be strongly affected by the network of hydrogen bonds interconnecting the molecules. These interactions are by far stronger than the interactions with the substrate. In a three-dimensional water assembly, each

molecule has the possibility to form four hydrogen bonds, two as donor molecule, through its own hydrogen atoms, and two as acceptor molecule, providing the O lone pair. This is what happens in the ice hexagonal lattice, where each molecule is tetrahedrally coordinated through the four hydrogen bonds. The network of hydrogen bonds in a two-dimensional water array is such that each molecule is involved in the formation of three hydrogen bonds, as donor and as acceptor. Those H atoms not involved in inter-molecular bonding either remain dangling or interact with the substrate. How hydrogen and hydrogen bonds are distributed depends on the relative orientation of the molecules and on the corrugation of the layer. In order to minimize the bias of the initial conditions on the final structure, in most of the cases a very unlikely starting orientation of the molecules has been selected, where all the molecules are perpendicular to the substrate, with one OH pointing to it and the second parallel. Afterwards, all the coordinates are relaxed, and the molecules rotate to maximize the intermolecular interaction and stabilize the structure.

For each model, in the initial configuration, the average height of the molecules over the substrate is 3 Å, but different initial height distributions have been tested: all O at the same height (h_0), sublattice A 0.3 Å higher (h_A), or sublattice B 0.3 Å higher ($h_{\rm B}$).

IV. RESULTS AND DISCUSSIONS

A. Water Monolayer on Free-standing Hexagonal BN

The only stable and ordered 2D array of water molecules with the M1 lattice is obtained by starting from the configuration h_B. As displayed in FIG. 2**a**, also in the optimized structure, the molecules of sublattice B are slightly higher (yellow O atoms in the figure). They are all parallel to the BN substrate, thus forming three hydrogen bonds with two neighboring molecules of sublattice A. The A molecules are 0.73 Å closer to the substrate and have a different orientation, such that one proton can form a hydrogen bond with a neighboring molecule, while the second H atom is pointing to the BN layer. Effective hydrogen-bonding with the substrate is possible only when the molecule is positioned on top of a N atom, and in this case, the O atom is even slightly closer to the BN substrate, i.e. 0.015 Å if compared to molecules above the BN ring-center and 0.07 Å than molecules on top of a B atom. The average height of the O atoms of sublattice A over BN is 3.37 Å. The O–O nearest neighbor distances are 2.6 Å, when an A molecule is the donor in the hydrogen bond, and 2.8 Å when it is the acceptor. Such differences in hydrogen bond lengths

are observed in all simulated structures, which is similar to previously called Kekulé type bond alternation. However, water molecules forming one hexagon are not equivalent, meanwhile two or even more different orientations are presented, which could be responsible for the deviation from a perfect shaped water hexagon. Besides, the existence of the *h*-BN substrate and the water lattice in different ice models are also crucial to the structure deformation, as clearly in most cases, corrugations between water in two layers are observed. In the final configuration, all molecules belonging to the same sublattice are equally oriented, thus the molecular dipoles sum up to a quite large in-plane value, i.e. 23.92 Debye per unit cell. The most relevant parameters characterizing this and the other optimized structures are reported in TABLE I.

All the optimizations starting from the M2 model result in a quite flat water overlayer, with corrugation smaller than 0.05 Å. In particular, the initial conditions h_0 and $h_{\rm B}$ give the same optimized structure, which is displayed in panel **b** of FIG. 2, whereas the structure depicted in panel **c** is obtained when starting from $h_{\rm A}$. In both cases, the molecules of one sublattice are parallel to the substrate and donate two hydrogen atoms to form hydrogen bonds with two neighboring molecules. The molecules in the other sublattice employ only one H atom to form one hydrogen bond with a neighboring molecule, while the second H atom is directed towards the substrate. In the first structure obtained from this model and named M2_topN, the molecules of sublattice A point to the N atoms of the BN layer and the corresponding O atoms are 3.27 Å above the substrate. In the second structure named M2_topC, the molecules pointing down are those of the B sublattice, which means that the H atom points to the center of the BN ring. The binding energy between water molecules and substrate is 0.015 eV stronger for the M2_topN than for the M2_topC, because in the former case the interaction is more effective. The M2 lattice is the least dense among those considered in this work, the overall intermolecular distance is quite large, around 2.9 Å. After the optimization, the O–O distances are distributed between values of 2.8 Å, when the molecule parallel to the substrate is the hydrogen bond acceptor, and 3.0 Å, when it is the donor.

In order to rule out biasing effects of the initial orientation of the molecules on the final structure, one optimization run has been started positioning most of the molecules parallel to the substrate. The resulting most stable final structure is also in this case the M2_topN configuration.

The M3 arrangement gives rise only to two different structures when in the initial configuration all the molecules are perpendicular to the surface. However, by selecting different orientations of the molecules that minimize the dipole moment, two more structures could be optimized. In FIG. 3 the four different structures are reported. In all the analyzed structures, the two sublattices lay at

different height over the substrate. The structure displayed in panel **a** of FIG. 3, and named M3_1, is characterized by having all the molecules belonging to one sublattice equally oriented, as it is also the case for the M1 and M2 structures described above. The A molecules are perpendicular to the substrate, forming a hydrogen bond with the closest N atom. The B molecules are parallel to BN (yellow in the figure), and both H atoms are employed in inter-molecular hydrogen bonds to neighboring molecules. The sublattice A is closer to BN, with an average distance between O and N of 3.31 Å. The height difference between the two sublattices is on average 0.91 Å.

The water molecules in the second optimized structure, M3_2 (panel **b**), can have four different orientations. In sublattice A, which is higher over the substrate, half of the molecules are parallel to the substrate and half are perpendicular to it, with one dangling hydrogen pointing upwards. These latter are 0.4 Å lower than the parallel molecules of the same sublattice. The molecules of sublattice B are closer to the substrate, at an average distance of 3.17 Å and are also distributed among two different kinds. Half of them is parallel to the substrate, but with the molecular dipole differently oriented with respect to the parallel A molecules, whereas the remaining molecules point towards the substrate and form hydrogen bonds to N atoms. The resulting distribution of the molecular dipoles minimizes the total dipole per unit cell, even though the in plane component is still quite large. Moreover, the M3_2 structure turns out to be the lowest in energy among all the water layers adsorbed on free-standing *h*-BN considered in this work.

A third structure has been obtained from an initial configuration where all the molecules are pointing upwards with one OH, while the other OH bonds are parallel to the BN substrate. The resulting structure, M3_3, is reported in FIG. 3**c**. It is also a bilayer, where the molecules of sublattice A are still perpendicular to the substrate and pointing upwards, while the B molecules are rotated to a parallel orientation with both hydrogen atoms forming hydrogen bonds with the neighboring molecules. The shortest O-BN distances are about 3.08 Å and the corrugation of the bilayer is about 0.89 Å. Since there is no direct interaction through hydrogen bonds to the substrate, the interaction energy computed for this structure is quite weak, $0.03 \sim 0.05$ eV lower per molecule.

The fourth structure based on model M3 is the M3_4, which is very similar to M3_1, but with different orientations of the molecular dipoles. The structure is reported in FIG. 3**d**. Thanks to this redistribution of the molecular orientation a significant reduction of the y component of the dipole moment is obtained with respect to M3_1. Other important parameters like adsorption energy, binding energy and corrugation are very similar to what was already obtained for the M3_1

structure.

TABLE I: Energetic and Structural Properties for Different Water Models: Interaction, Adsorption and H-bond Energy, Corrugation between Two Water Layers, Oxygen-Oxygen Distance, and Dipole Moment per Unit Cell[a]

	Energy (eV)			corrugation (Å)	d_{O-O} (Å)	Dipole moment (D)			
	E_{int}	E_{ads}	$E_{H\text{-}bond}$			μ_x	μ_y	μ_z	$\lvert\mu\rvert$
M1	-0.050	-0.434	-0.256	0.73	2.6, 2.8	17.26	16.56	-5.84	24.62
M2_topN	-0.070	-0.433	-0.242	0.03	2.8, 3.0	8.60	-5.08	-1.08	10.05
M2_topC	-0.055	-0.418	-0.242	0.05	2.8, 3.0	8.78	4.92	-1.23	10.14
M3_1	-0.053	-0.421	-0.245	0.91	2.6, 2.8	6.04	-10.91	-3.07	12.85
M3_2	-0.053	-0.458	-0.270	0.77, 1.15	2.6, 2.7, 2.8	8.57	-5.31	-0.25	10.08
M3_3	-0.023	-0.390	-0.245	0.80	2.6, 2.8	6.31	-0.23	-2.62	6.84
M3_4	-0.053	-0.418	-0.243	0.87	2.6, 2.8	6.12	-0.01	-3.04	6.83
M4	-0.062	-0.429	-0.245	0.90	2.6, 2.8	0.03	-0.08	-3.02	3.02

[a] Number of water molecules and the *h*-BN area in each unit cell: M1: 8 water molecules / 71.49 Å^2; M2: 4 water molecules / 44.00 Å^2; M3 and M4: 4 water molecules / 33.00 Å^2.

We are looking for the molecular arrangement that could best represent the nano-ice cluster observed in the pore of the nanomesh by STM imaging. From the binding energy computed for the described structures, it is not possible to identify an outstanding structure that is significantly more stable than the others. Excluding the M3_2 structure, which is the only one not forming any hydrogen bond with the substrate, the adsorption energies are within 0.04 eV per water molecule. The adsorption energy is dominated by the intermolecular hydrogen bonding ($E_{H\text{-}bond}$). Each hydrogen bond contributes more than the interaction with the BN surface (E_{int}). The hydrogen bond energy is in most of the cases around -0.25 eV, with one exception for the M3_2 structure, for which the average hydrogen bonding is more effective with an average energy of -0.27 eV. Stronger hydrogen bonds can be related to the presence of dangling H and a better height distribution of molecules with different orientation. This structure is overall also the lowest in energy and therefore one of the best candidates for the nano-ice cluster. However, the experimental analysis seems to indicate that the O are distributed over two layers, which would exclude the M3_2, but also all the M2 structures, which show no corrugation at all. Also the other structures that have been described are not very probable due to the large in plane dipole moments (see the data in the TABLE I).

Therefore a new model was generated which is still based on the M3 distribution of the O atoms over the substrate, which looks to be the most stable since each molecule is approximately on top of one N atom. The unit cell of the new model is a 2×3 supercell containing 24 water molecules with six different orientations of the molecular dipoles, thus minimizing the total dipole moment. The resulting optimized structure M4 is reported in FIG. 4. The molecules of the two sublattices are distributed over two layers, where the lowest molecules are perpendicular to the surface, with an average O-BN distance of 3.30 Å, each forming one hydrogen bond with the N atom beneath. The other molecules are displaced 0.9 Å higher over the substrate and are parallel to the substrate, with both H atoms forming hydrogen bonds with neighboring molecules. As expected, the x and y dipole components are almost zero, while there is still a contribution along z due to the downwards orientation of half of the molecules. Moreover, the adsorption energy is one of the lowest among those computed on free-standing BN. Therefore, we consider this low-dipole structure as our best candidate to represent the nano-ice cluster reported from experiment.

B. Water Cluster on the Nanomesh

The optimization and characterization of the nanomesh superstructure with our computational set up has been already described in previous works[3]. Here we use a slab of four 12×12 Rh layers surmounted by a 13×13 BN overlayer. By standard structure optimization, the overlayer corrugates and forms the characteristic pore and wire regions, where the pore is a hexagonal-shaped depression of about 2 nm of diameter. 38 molecules have been extracted from the optimized M4 overlayer and have been collocated over the nanomesh, thus covering the whole pore. The initial average height of the O with respect to the topmost Rh layer is about 5.5 Å. The atomic configurations before and after the optimization are reported in FIG. 5**a** and **b**, respectively. It is observed that the structure optimization induces the reorientation of some water molecules close to the rim of the nanomesh. Indeed, the molecules at the edge of the cluster have dangling H. It is then energetically favorable to redirect the corresponding OH towards the substrate and form additional hydrogen bonds. On the other hand, the rearrangement induces a neat increase of the total dipole of the cluster, which in the final configuration is 7.95, 17.16, and 12.42 D in x, y and z directions, respectively. The total interaction energy and the adsorption energy are -0.112 and -0.482 eV. The molecules at the border of the cluster typically are single acceptor and single donor in terms of the interaction with the neighboring molecules. The second OH not involved in

water-water hydrogen bonding is free to rotate. When the condition are such that the formation of a hydrogen bond with a N of the substrate is possible, the molecule gets closer to the substrate and the typical N–H distance is around 2.5 Å, corresponding to a quite weak interaction. Being these interactions with the substrate quite weak, several molecules remain with a dangling hydrogen. The potential energy surface along the rotation angle of these molecules is quite flat, therefore the optimization algorithm may have some difficulties in finding a global minimum. The two dimensional cluster is anyway stabilized by the interaction with the substrate. The same cluster in gas phase is, indeed, not stable and tends to a three dimensional aggregate, where each molecule has the possibility to be three or four coordinated with other molecules.

The actual number of water molecules in the pore might also affect the final structure. From the experimental data we know that there should be (20±5) per layer[6], therefore 38 molecules is in the right range. It is even possible that molecules move fast from the cluster to the wire and in the opposite direction, thus changing the conditions at the rim. The presence of molecules on the wire is quite probable, and they could play a role in stabilizing the cluster in the pore. However, these molecule could never be imaged by STM, which is perfectly consistent with fast motion of molecules, weakly interacting with the substrate.

As already observed for the water arrays on free-standing BN, the O–O distances are not all the same. In the center of the cluster, the O–O distance is 2.62 Å if the hydrogen bond acceptor is a molecule parallel to the substrate, whereas it is longer, 2.83 Å, if the acceptor is a molecule interacting with the substrate through its second H, and therefore shifted downwards. Namely, the O atoms of the perpendicular molecule is at about 5.5 Å from the topmost Rh layer, while the other molecules are about 0.8 Å higher. For the molecules at the rim the differences in the O–O distance are smaller, 2.68 Å and 2.79 Å, respectively. The optimized structure reproduces the corrugation of the bilayer nano-ice cluster observed in the experiment. The height difference between the water molecules of the two sublattices is appearing in the STM images (FIG. 5**c**) as difference in brightness, which is consistent with the interpretation from the experimental analysis. The contrast modulation is more evident in the center of the cluster, whereas, at border where some molecules are rotated, the image becomes more blurred. When the orientation of the molecule is such that the O lone pair is not completely accessible from above, the STM imaging cannot clearly detect the molecular density, and the corresponding area becomes darker. Therefore, at the rim, some of the molecules appear as darker smaller spots or become even invisible.

V. CONCLUSION

In this work, we investigated different models of water molecule assembly adsorbed on BN, which could reproduce the atomic structure of the experimentally observed nano-ice cluster. The proposed initial configurations present similar characteristics in terms of number of molecules per unit, type and number of intermolecular interactions, distance from the substrate, and 2D hexagonal arrangement. The geometry optimizations carried out on flat BN surface lead to structures that are all consistent with a bilayer water lattice as observed in experiment. The intermolecular distances and the adsorption energy do not provide strong arguments to prefer one structure over the others, making one exception for the model M2, which has to be discarded due to the too large intermolecular distance. The distribution of molecular dipole, however, changes significantly from cluster to cluster. We then conclude that the M4 cluster should be the most probable arrangement of water molecules on BN, since by orienting the six molecules forming the hexagonal units in six different ways, the total dipole is minimized. In ref. [6], we already showed that 42 water molecules extracted from the M4 model, without any relaxation, generate a local modulation of the electrostatic potential which closely resembles the experimental observation. Here, 38 M4 water molecules are optimized in the pore of the nanomesh, and the simulated STM image are in agreement with the experiment, where spots of different brightness identify molecules at different height.

For the system addressed in this work, it is especially interesting to consider the molecular dipole distribution, which has a crucial role in discriminating among structures that otherwise would have similar adsorption properties. This is clearly important to understand the formation of stable structure in the pore of the nanomesh, but could also be a useful criterion on other templated substrate where modulation of the electrostatic potential are present.

Acknowledgment

The authors thank Prof. Dr. Thomas Greber and Dr. Haifeng Ma for fruitful discussions. This work is supported by Swiss National Science Foundation under Grant No. CRSI20_122703. Generous computational resources from Swiss National Supercomputer Centre (CSCS) and University of Zurich are gratefully acknowledged.

References

[1] M. Corso, W. Auwärter, M. Muntwiler, A. Tamai, T. Greber, and J. Osterwalder. Boron Nitride Nanomesh. *Science*, 303(5655):217–220, 2004.

[2] S. Berner, M. Corso, R. Widmer, O. Groening, R. Laskowski, P. Blaha, K. Schwarz, A. Goriachko, H. Over, S. Gsell, M. Schreck, H. Sachdev, T. Greber, and J. Osterwalder. Boron nitride nanomesh: Functionality from a corrugated monolayer. *Angewandte Chemie-International Edition*, 46(27):5115–5119, 2007.

[3] Y. Ding, M. Iannuzzi, and J. Hutter. Investigation of boron nitride nanomesh interacting with water. *Journal of Physical Chemistry C*, 115(28):13685–13692, 2011.

[4] O. Bunk, M. Corso, D. Martoccia, R. Herger, P. R. Willmott, B. D. Patterson, J. Osterwalder, J. F. van der Veen, and T. Greber. Surface x-ray diffraction study of boron-nitride nanomesh in air. *Surface Science*, 601(2):L7–L10, 2007.

[5] R. Widmer, S. Berner, O. Gröning, T. Brugger, J. Osterwalder, and T. Greber. Electrolytic in situ stm investigation of h-bn-nanomesh. *Electrochemistry Communications*, 9(10):2484–2488, 2007.

[6] H. F. Ma, T. Brugger, S. Berner, Y. Ding, M. Iannuzzi, J. Hutter, J. Osterwalder, and T. Greber. Nano-ice on boron nitride nanomesh: Accessing proton disorder. *ChemPhysChem*, 11(2):399–403, 2010.

[7] Y. Ding, M. Iannuzzi, and J. Hutter. Investigation of h-bn/rh(111) nanomesh interacting with water and atomic hydrogen. *Chimia*, 65(4):256–259, 2011.

[8] H. F. Ma, Y. Ding, M. Iannuzzi, T. Brugger, S. Berner, J. Hutter, J. Osterwalder, and T. Greber. Chiral distortions of confined ice hexamers. Submitted.

[9] D. L. Doering and T. E. Madey. The adsorption of water on clean and oxygen-dosed Ru(001). *Surface Science*, 123(2-3):305–337, 1982.

[10] M. A. Henderson. The interaction of water with solid surfaces: fundamental aspects revisited. *Surface Science Reports*, 46(1-8):1–308, 2002.

[11] H. Ogasawara, B. Brena, D. Nordlund, M. Nyberg, A. Pelmenschikov, L. G. M. Pettersson, and A. Nilsson. Structure and bonding of water on Pt(111). *Physical Review Letters*, 89(27):276102, 2002.

[12] A. Michaelides, A. Alavi, and D. A. King. Different surface chemistries of water on Ru$\{0001\}$: From

monomer adsorption to partially dissociated bilayers. *Journal of the American Chemical Society*, 125(9):2746–2755, 2003.

[13] J. Cerdá, A. Michaelides, M. -L. Bocquet, P. J. Feibelman, T. Mitsui, M. Rose, E. Fomin, and M. Salmeron. Novel water overlayer growth on Pd(111) characterized with scanning tunneling microscopy and density functional theory. *Physical Review Letters*, 93(11):116101, 2004.

[14] T. Schiros, S. Haq, H. Ogasawara, O. Takahashi, H. Öström, K. Andersson, L. G. M. Pettersson, A. Hodgson, and A. Nilsson. Structure of water adsorbed on the open Cu(110) surface: H-up, H-down, or both? *Chemical Physics Letters*, 429(4-6):415–419, 2006.

[15] A. Verdaguer, G. M. Sacha, H. Bluhm, and M. Salmeron. Molecular structure of water at interfaces: Wetting at the nanometer scale. *Chemical Reviews*, 106(4):1478–1510, 2006.

[16] A. Michaelides and K. Morgenstern. Ice nanoclusters at hydrophobic metal surfaces. *Nature Materials*, 6(8):597–601, 2007.

[17] J. Carrasco, A. Michaelides, M. Forster, S. Haq, R. Raval, and A. Hodgson. A one-dimensional ice structure built from pentagons. *Nature Materials*, 8(5):427–431, 2009.

[18] T. Schiros, H. Ogasawara, L. -Å. Naślund, K. J. Andersson, J. Ren, Sh. Meng, G. S. Karlberg, M. Odelius, A. Nilsson, and L. G. M. Pettersson. Cooperativity in surface bonding and hydrogen bonding of water and hydroxyl at metal surfaces. *Journal of Physical Chemistry C*, 114(22):10240–10248, 2010.

[19] CP2K version 2.2.426 (Release Version), the CP2K developers group (2012). CP2K is freely available from http://www.cp2k.org.

[20] G. Lippert, J. Hutter, and M. Parrinello. A hybrid gaussian and plane wave density functional scheme. *Molecular Physics*, 92(3):477–487, 1997.

[21] J. P. Perdew, K. Burke, and M. Ernzerhof. Generalized gradient approximation made simple. *Physical Review Letters*, 77(18):3865–3868, 1996.

[22] Y. K. Zhang and W. T. Yang. Comment on "generalized gradient approximation made simple". *Physical Review Letters*, 80(4):890–890, 1998.

[23] S. Grimme. Semiempirical gga-type density functional constructed with a long-range dispersion correction. *Journal of Computational Chemistry*, 27(15):1787–1799, 2006.

[24] S. Goedecker, M. Teter, and J. Hutter. Separable dual-space gaussian pseudopotentials. *Physical Review B*, 54(3):1703–1710, 1996.

[25] C. Hartwigsen, S. Goedecker, and J. Hutter. Relativistic separable dual-space gaussian pseudopoten-

tials from h to rn. *Physical Review B*, 58(7):3641–3662, 1998.

[26] M. Krack. Pseudopotentials for h to kr optimized for gradient-corrected exchange-correlation functionals. *Theoretical Chemistry Accounts*, 114(1-3):145–152, 2005.

[27] J. VandeVondele and J. Hutter. Gaussian basis sets for accurate calculations on molecular systems in gas and condensed phases. *Journal of Chemical Physics*, 127:114105, 2007.

[28] S. F. Boys and F. Bernardi. Calculation of small molecular interactions by differences of separate total energies - some procedures with reduced errors. *Molecular Physics*, 19(4):553, 1970.

[29] J. Tersoff and D. R. Hamann. Theory and application for the scanning tunneling microscope. *Physical Review Letters*, 50(25):1998–2001, 1983.

[30] J. Tersoff and D. R. Hamann. Theory of the scanning tunneling microscope. *Physical Review B*, 31(2):805–813, 1985.

[31] N. Marzari and D. Vanderbilt. Maximally localized generalized wannier functions for composite energy bands. *Physical Review B*, 56(20):12847–12865, 1997.

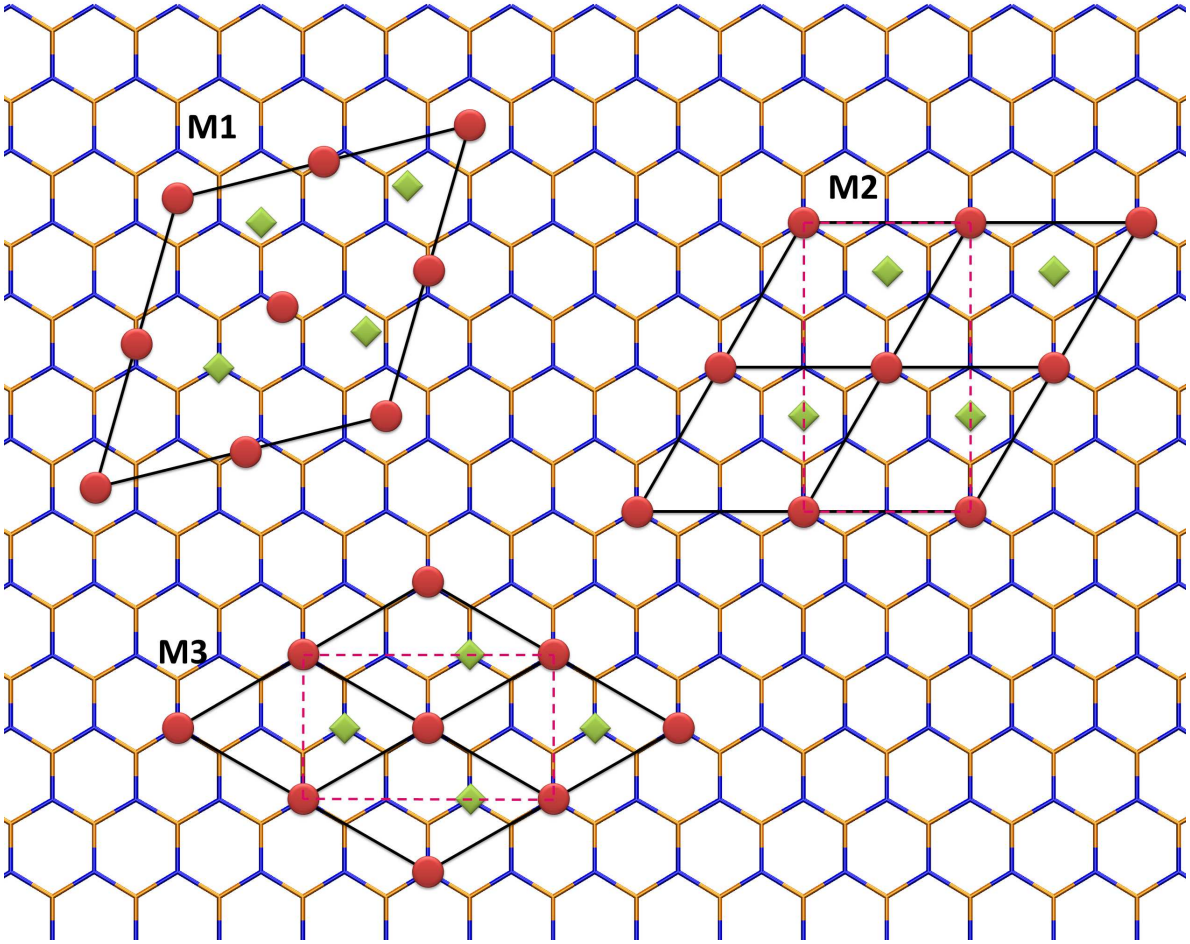

FIG. 1: Different water cluster lattices. Only the position of the O atoms are considered here and the water molecules are represented by the red circles and green squares as in different water layer. The black lines give the unit cell in each model, while in M2 and M3 the hexagonal unit cells are converted to orthogonal ones as indicated by the magenta dash lines used in the calculations. The thin line in the background are BN monolayer, with B in orange and N in blue.

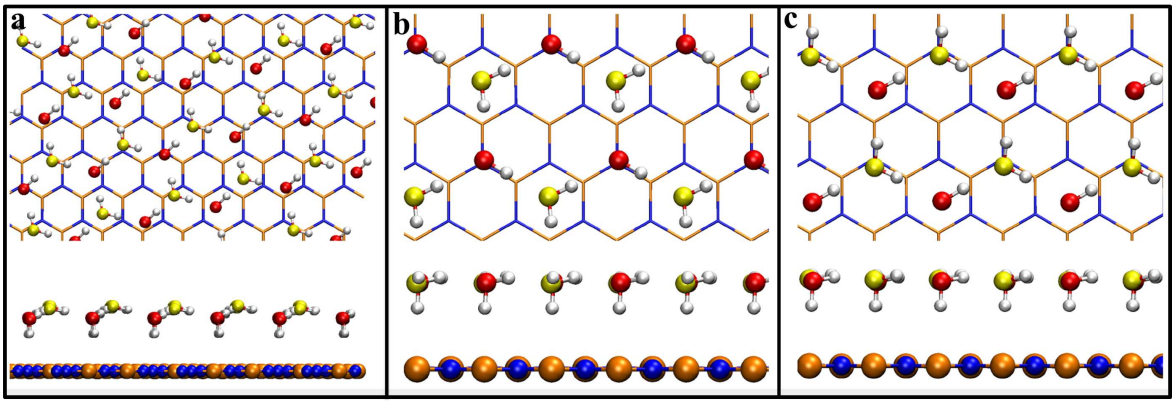

FIG. 2: Top and side view of different water clusters adsorbed on a flat BN surface. In the ball and stick representation of the structure, the red and yellow spheres are oxygen atoms in different layer, while white for H, blue for N and orange for B, respectively. The BN monolayer is given by the thin lines forming the honey-comb lattice in the top view with the same color scheme. **a**. Model M1. **b**. Model M2_topN. **c**.Model M2_topC.

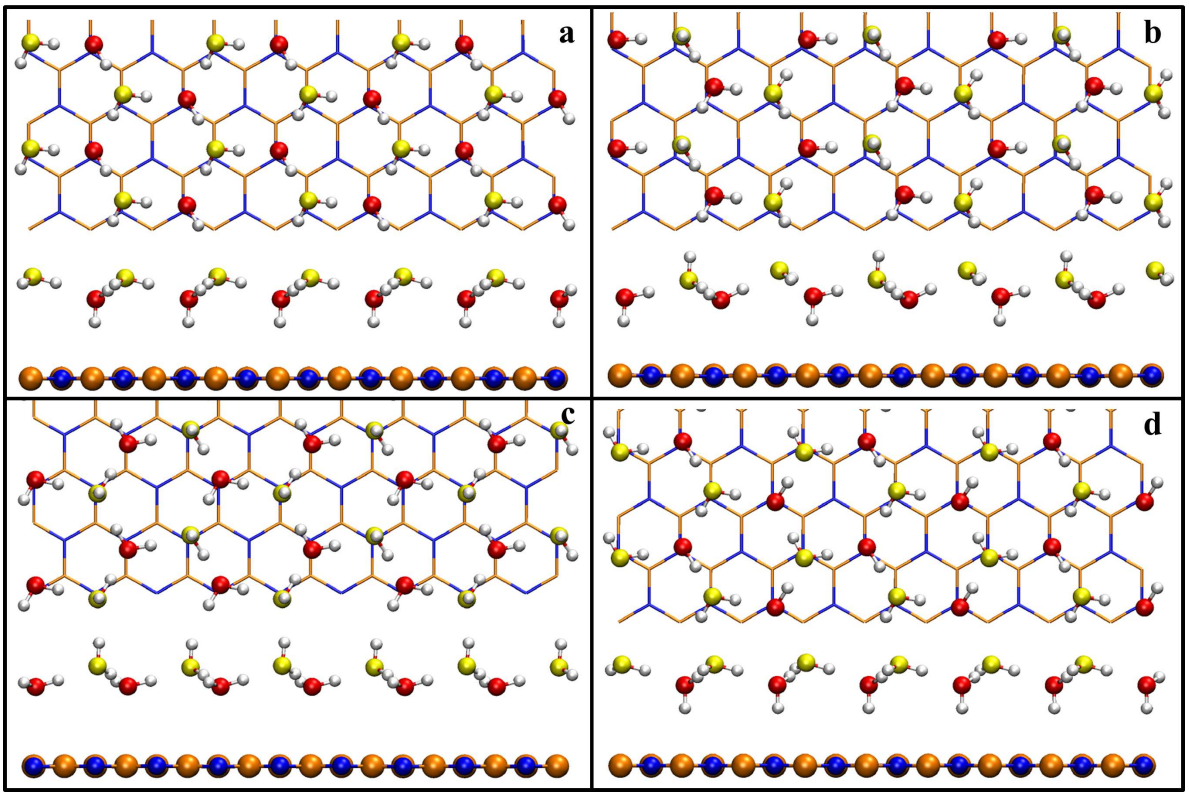

FIG. 3: Top and side view of different water clusters adsorbed on a flat BN surface. **a**. Model M3_1. **b**. Model M3_2. **c**. Model M3_3. **d**. Model M3_4. See caption of FIG. 2 for the representation of the molecules.

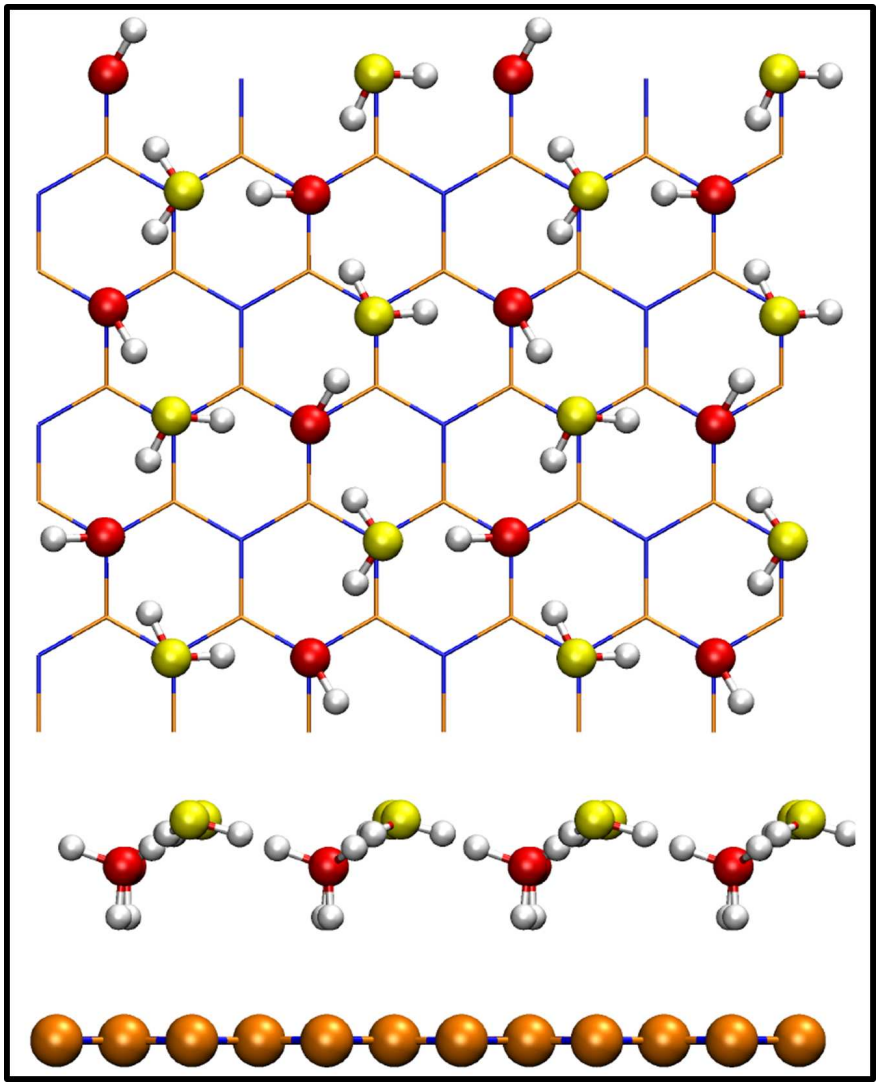

FIG. 4: Top and side view of model M4 adsorbed on a flat BN surface. See caption of FIG. 2 for the representation of the molecules.

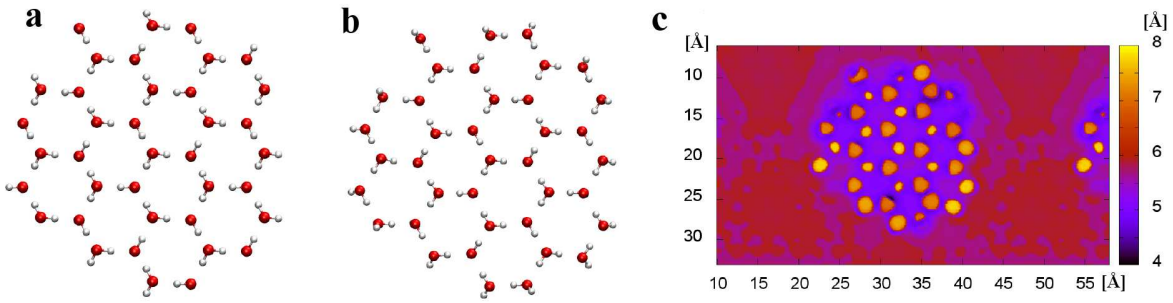

FIG. 5: Top view of the 38 water molecules optimized in the pore of the nanomesh (**a**. before geometry optimization; **b**. after geometry optimization) and the corresponding STM topography images (**c**) for the optimized structure. The ball and stick representations are used for the water molecule, with the oxygen in red and hydrogen in white, respectively.